Available online at www.sciencedirect.com
ScienceDirect
Journal of Magnetic Resonance 186 (2007) 273–281
JMR Journal of Magnetic Resonance
www.elsevier.com/locate/jmr

An optimization method for designing SENSE imaging RF coil arrays

Gang Chen *, L. Tugan Muftuler, Seung H. Ha, Orhan Nalcioglu

Tu & Yuen Center for Functional Onco-Imaging, University of California, Irvine, CA 92697, USA

Received 27 October 2006; revised 13 January 2007
Available online 24 March 2007

Abstract

An optimization method in RF coil array design for SENSE imaging is described. Using this method the optimized RF coil geometries can be calculated numerically given the required SENSE imaging performance. Although this method can be applied to optimize the RF coil arrays for both 1D and 2D SENSE imaging, to demonstrate the potential applications of this method, we designed RF coil arrays for 2D SENSE imaging and compared their performance by simulation. An optimized 4-channel receive-only RF coil array designed for 2D SENSE imaging was implemented and tested to demonstrate the feasibility of the proposed technique. Imaging results showed reasonable agreement with the simulations, thus the method can be applied to RF coil array designs for SENSE imaging when optimum imaging performance is desired.

Keywords: SENSE imaging; Optimized RF coil array

1. Introduction

Sensitivity encoding (SENSE) [1] is a parallel imaging technique that reduces MR scanning time by under sampling k-space in the phase encoding direction and reconstructing the aliased images with RF (radio frequency) coil sensitivity information in the image domain. In addition to the intrinsic signal-to-noise ratio (SNR) loss by a factor of $\sqrt{R}$, where the phase encoding steps are reduced by a factor of R, there always exists an additional SNR loss due to the noise correlation between the RF coils detecting the signal from the same sample volume where thermal noise is generated. Furthermore the SNR distribution in the SENSE images acquired with non-optimized RF coil arrays is usually non-uniform, i.e. the SNR in the central region and the peripheral regions of the sample far away from the coils is usually lower than in the peripheral regions close to the coils.

The importance of designing optimized RF receiver coil arrays for SENSE imaging has been recognized for several years. Optimization of RF coil array design for SENSE imaging is important because the physical layout of the RF coil arrays determines the electromagnetic field generated by the coils, which dramatically affects the final SNR in SENSE imaging. Therefore, various coil array designs have been investigated for optimized SENSE imaging performance [2–4]. In these methods, a finite number of RF coil array designs were simulated for SENSE imaging, and the best design was then chosen as the optimized design or as a standard to apply to other similar designs. However, the SNR in SENSE imaging is so sensitive to coil array designs that studying only a finite number of designs is insufficient to find the SENSE-optimized design or to determine any set of optimum parameters that can be generically used.

Recently, computerized optimization processes in designing optimized RF coil arrays have been published [5–10]. In [9] the size of the coil was optimized and in [10] the positions of a set of fixed-shape coils were optimized. In our previous work [5,6] the elements of an RF coil array were modeled by a continuous surface current density, and the current distributions were optimized for improved SENSE imaging performance. The resulting continuous surface current distributions were discretized and

* Corresponding author. Fax: +1 949 824 3481.
E-mail address: gangc@uci.edu (G. Chen).

1090-7807/$ - see front matter © 2007 Elsevier Inc. All rights reserved.
doi:10.1016/j.jmr.2007.03.014

simplified to achieve a practical RF coil design. The advantage of this method is that the surface current density can assume any arbitrary distribution for optimum performance. However, the resulting coil elements might require multiple parallel branches, and it becomes difficult to obtain the correct current distribution among those branches. On the other hand, in [7,8] the RF coil arrays were modeled by a set of connected conductor segments and the locations of the vertices of these segments were optimized. In this approach, parallel branches are avoided and the solution is restricted to coil elements with single wire loops of arbitrary geometries. Wire crossing without short circuiting is allowed so that butterfly shapes are possible. This second approach is described in detail in this manuscript. The common goal in all these recent methods is to solve an inverse problem to find a coil topography that achieves better SENSE imaging performance, so that the final coil topography is more likely to approach optimum SENSE operation.

Wiesinger et al. [11] has studied what the ultimate SNR in SENSE imaging would be. In their study the ultimate SNR achievable by the ideal electromagnetic field was studied. Although the ultimate RF coil array design was not studied, the results can be used to set the stopping criteria when optimizing RF coil arrays, i.e. when the SENSE SNR of an RF coil array being optimized is within a certain range of the ultimate SNR, the optimization process stops and returns this optimized design.

In this paper, a robust optimization method is presented for designing the RF coil arrays for SENSE imaging. The RF coil geometry was modeled by a set of connected conductor segments. Then, the SENSE imaging SNR was formulated as a function of the RF coil geometry, and a solution was sought in the least squares sense to find the most efficient coil array design. Various target volumes were defined for the optimization, and the optimized coil array designs were compared by simulation. The approach outlined here yielded more efficient RF coil array designs compared with a previous optimized design. One of the optimized RF coil arrays was built; and RF coil sensitivity and SENSE imaging SNR were measured and compared with the simulation results. These experiments verified the accuracy of the simulation. The feasibility of 2D (two dimensional) SENSE imaging using the optimized RF coil array was verified by imaging a resolution phantom, and the reconstructed 2D SENSE images showed minimum artifacts even at the full acceleration rate (when phase encoding reduction factor equals the number of coil elements).

2. Materials and methods

2.1. Coil modeling and field calculation

RF coils can be used to detect a MRI signal because the RF wave generated by precessing spins induces alternating current in the surrounding conductive wires. These metal segments are usually connected to form a closed loop (shown in Fig. 1) near the imaging volume to efficiently detect the RF signal. When the metal segments are connected to form an RF coil, the coil is fully determined by the locations of the joint vertices $\{r_i\}_\gamma$ of all the metal segments (γ is the index of the RF coils). Thus $\{r_i\}_\gamma$ can be used to model the RF coil geometries. In order to find the most efficient coil shape in SENSE imaging, the $\{r_i\}_\gamma$ can be treated as unknowns, and an inverse problem can be solved to find the best coil shape to achieve improved SNR performance for different SENSE imaging purposes.

Once the coil geometries are defined by $\{r_i\}_\gamma$ as described above, the next step is to calculate the magnetic field generated by the RF coil loop. This is necessary for calculating the SENSE SNR achievable by the RF coil array. The electromagnetic field can be calculated by solving the full Maxwell equations using finite-difference time-domain approaches [12,13], finite element approaches [14,15], or integral equation solvers [16], and can also be calculated under quasistatic approximation [17–19] using the Biot–Savart law when the RF coil size and imaging volume are small compared to the RF wavelength. Using either method, the magnetic field distribution can be determined by the coil structure and a given load. Therefore, $B_\gamma(\rho_j, \{r_i\}_\gamma)$ can be found, which gives the magnetic field at location ρ_j generated by the RF coil loop γ that is determined by $\{r_i\}_\gamma$.

2.2. SNR calculation

Because SNR is one of the most important factors that determine the SENSE image quality, one needs to formulate the SNR in terms of the magnetic field in order to find the optimized RF coil array topography. In order to calculate the SNR in SENSE imaging (SNR_{SENSE}) given the magnetic field distribution, we followed the same steps in [3,5,20]. The receiver noise matrix Ψ is approximated by summing the scalar product of coil sensitivities over a number of points ρ_j inside the sample.

$$\Psi_{\gamma,\gamma'} = \sum_{j=1}^{N} B_\gamma(\rho_j) \cdot B_{\gamma'}(\rho_j) \tag{1}$$

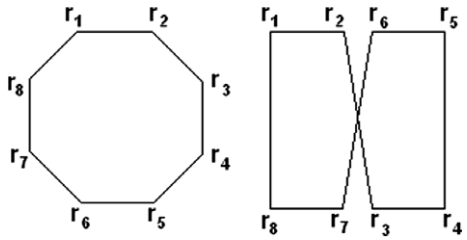

Fig. 1. The basic geometries of RF coil elements that make up the RF coil array. The geometry of each element is determined by a set of indexed vertices $\{r_i\}_\gamma$.

Here, $B_\gamma(\rho_j)$ is the field generated by the γth coil at point ρ_j and $B_{\gamma'}(\rho_j)$ is the field generated by the γ'th coil at the same point.

$\mathrm{SNR}_{\mathrm{full},\rho}$, the SNR at point ρ when the image is taken with full phase encoding without SENSE acceleration, is calculated by Eq. (2),

$$\mathrm{SNR}_{\mathrm{full},\rho} = \sqrt{\Sigma_\rho^H \cdot \Psi^{-1} \cdot \Sigma_\rho} \tag{2}$$

where Σ_ρ is the vector containing the complex sensitivity of every coil element at location ρ.

The geometry factor (or g-factor) at location ρ is calculated by Eq. (3)

$$g_\rho = \sqrt{((S^H \cdot \Psi^{-1} \cdot S)^{-1})_{\rho,\rho}(S^H \cdot \Psi^{-1} \cdot S)_{\rho,\rho}} \tag{3}$$

Here S is the coil sensitivity matrix (H indicates transposed complex conjugate) at the effective superimposed positions related to location ρ.

Finally the $\mathrm{SNR}_{\mathrm{SENSE}}$ at point ρ is calculated by,

$$\mathrm{SNR}_{\mathrm{SENSE},\rho} = \mathrm{SNR}_{\mathrm{full},\rho}/(g_\rho \cdot \sqrt{R}) \tag{4}$$

Here, R is the reduction factor of the phase encoding steps.

As an example of a 2D $\mathrm{SNR}_{\mathrm{SENSE}}$ calculation, to find the $\mathrm{SNR}_{\mathrm{SENSE}}$ of voxel "a" as shown in Fig. 2 from a given 4-channel RF array, first Ψ and the $\boldsymbol{B}$ field at every voxel in the volume that generates noise is calculated using Eq. (1). Second, the full SNR at voxel "a" ($\mathrm{SNR}_{\mathrm{full,a}}$) is calculated using Eqs. (2) and (5). Third, the voxels that are superimposed with voxel "a" in 2D SENSE imaging are located (in this case voxels "b, c" and "d"), then the g-factor is calculated using Eqs. (3) and (6). Finally the $\mathrm{SNR}_{\mathrm{SENSE}}$ of voxel "a" is calculated using Eq. (4).

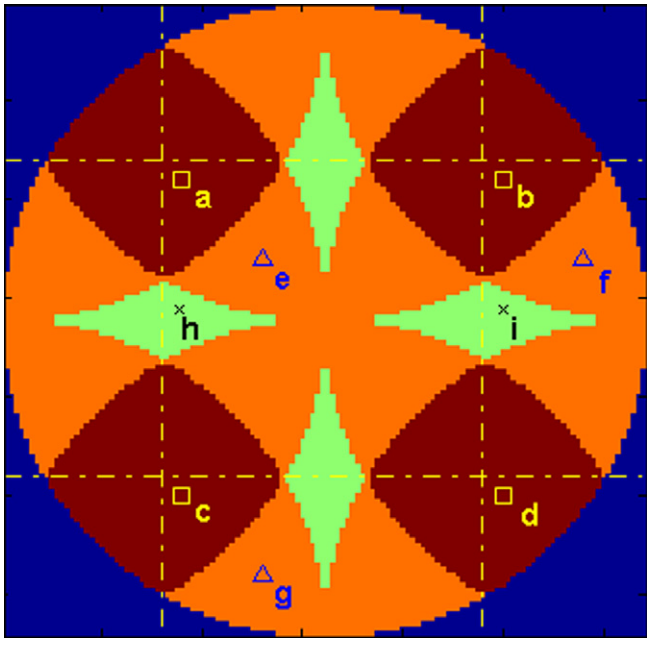

Fig. 2. Schematic of 2D Cartesian SENSE imaging with 2×2 reductions in two phase encoding directions for a cross section of a cylindrical object. Not all of the voxels have 4 times aliasing because of the shape of the object. Voxels with 4, 3, and 2 times aliasing are shown with dark red, orange, and green color, respectively. (For interpretation of the references to colour in this figure legend, the reader is referred to the web version of this article.)

$$\Sigma_{\mathrm{a}} = \begin{pmatrix} B_1(\mathrm{a}) \\ B_2(\mathrm{a}) \\ B_3(\mathrm{a}) \\ B_4(\mathrm{a}) \end{pmatrix} \tag{5}$$

$$S = \begin{pmatrix} B_1(\mathrm{a}) & B_1(\mathrm{b}) & B_1(\mathrm{c}) & B_1(\mathrm{d}) \\ B_2(\mathrm{a}) & B_2(\mathrm{b}) & B_2(\mathrm{c}) & B_2(\mathrm{d}) \\ B_3(\mathrm{a}) & B_3(\mathrm{b}) & B_3(\mathrm{c}) & B_3(\mathrm{d}) \\ B_4(\mathrm{a}) & B_4(\mathrm{b}) & B_4(\mathrm{c}) & B_4(\mathrm{d}) \end{pmatrix} \tag{6}$$

It should be noted that the superposition in SENSE imaging depends on the shape of the object to be imaged. For example, the voxel at location "e", is only superimposed with the voxels at locations "f" and "g" in 2D SENSE imaging. When the g-factor of voxel "e" is calculated, the sensitivity matrix should only include the sensitivities of voxels "e, f" and "g". Similarly, when the g-factors of voxels "h" and "i" are calculated, the sensitivity matrix only includes the sensitivities of these voxels.

2.3. Coil optimization

Once the SENSE SNR of every voxel in the VOI (volume of interest) is formulated as a function of magnetic field and the magnetic field is formulated as a function of RF coil geometry, the SENSE SNR of any given voxel ρ can be formulated as a function of RF coil geometry, which is given as $\mathrm{SNR}_{\mathrm{SENSE},\rho}(\{\{r_i\}_\gamma\})$.

In order to apply optimization algorithms to find efficient RF coil array designs for SENSE imaging, a cost function that evaluates the performance of the RF coil array design needs to be given. Depending on the applications of RF coil array design, different weights w_{ρ_j} can be given to the $\mathrm{SNR}_{\mathrm{SENSE}}$ of different voxels. If the RF coil array design will be used for SENSE imaging with different acceleration factors R_m, different weights w_{R_m} for each acceleration factors can also be assigned to achieve a design suitable for multipurpose SENSE imaging. Therefore the cost function will have the general form given in Eq. (7).

$$O = O\{\{r_i\}_\gamma, w_{\rho_j}, R_m, w_{R_m}\} \tag{7}$$

Finally, an optimization algorithm can be applied to find the locations of the coil vertices $\{r_i\}_\gamma$ that would minimize the cost function, and the resulting RF coil arrays can be constructed according to the optimization results.

3. Results

3.1. Coil optimization

Using the optimization method described above, 4-channel RF coil arrays for 2D SENSE imaging with a

2×2 acceleration rate along two phase encoding directions were designed for imaging the human head at 1.5 T. The head shape was assumed to be a simple cylinder with a 22.4 cm diameter and 22.4 cm length. The VOI was the central part of the cylinder with the same diameter as the head and a 13.4 cm length. The RF coil array was confined on a cylindrical surface with a 28 cm diameter. Each coil element was modeled by 8 vertices as shown in Fig. 1. The vertices were allowed to move freely on the 28 cm cylindrical surface in the optimization process. The number of vertices was chosen empirically to minimize redundancy while maintaining generality. Symmetry along the two phase encoding directions was utilized to speed up the calculation. Iterations were done on a single coil element and the coil geometry was mirrored in the other three quadrants to update the geometries of the remaining three coils.

Since the RF coil size and imaging volume are small compared with the RF wavelength at 1.5 T, the RF coils can be simulated under quasistatic approximation [17–19]; therefore we calculate the magnetic field of the RF coils using the Biot–Savart law (here the sample loading is ignored). Since the $\{r_i\}_\gamma$ are the unknowns, we formulate the magnetic field generated by each segment as a function of $\{r_i\}_\gamma$ using the Biot–Savart law. The net magnetic field of the whole loop can be calculated by superimposing the magnetic field of each segment.

Since the goal is to maximize the overall $\mathrm{SNR}_{\mathrm{SENSE}}$, the cost function given in Eq. (8) was chosen. The $\mathrm{SNR}_{\mathrm{SENSE}}$ was sampled within the volume of interest with 1 cm isotropic resolution, where N is the total number of points sampled.

$$O\{\{r_i\}_\gamma\} = \sum_j^N \frac{1}{\mathrm{SNR}^2_{\mathrm{SENSE},\rho_j}(\{r_i\}_\gamma)} \tag{8}$$

The optimization program was developed under the MATLAB™ environment, and the built-in FMINSEARCH function was used to find the local minima of the cost function. FMINSEARCH uses a multidimensional unconstrained nonlinear minimization (Nelder-Mead). It tries to find the minimum of a scalar function of several variables, starting at an initial estimate. It takes about 10 min to find the local minimum with one random initial location. The process was repeated with different random initial locations for three days on three computers until the solutions calculated by the three computers converged to the same minimum. The efficiency of the method can be improved by using the clustering method, the simulated annealing method, or genetic algorithms as discussed in [21].

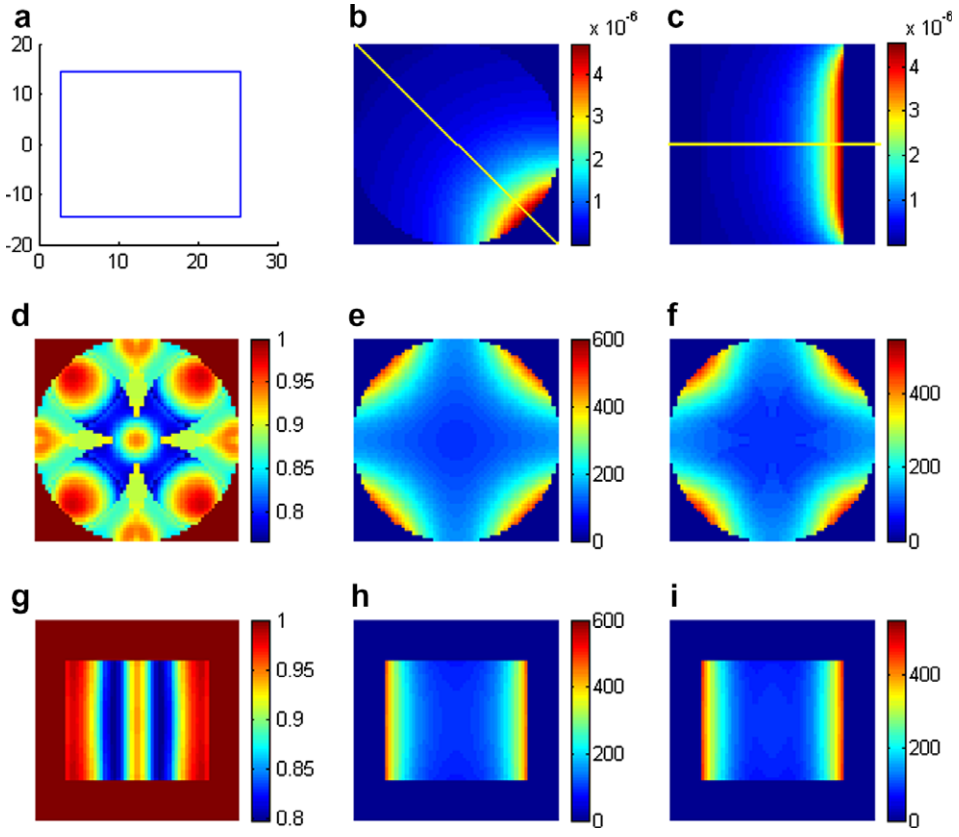

Fig. 3. The rectangular coil design found in the literature. The geometry of one of the RF coil array elements (a). When the head is modeled by a cylinder, the coil sensitivity profiles through the center slice and the diagonal slice are shown by (b) and (c). The yellow lines in (b) and (c) represent the locations of the diagonal slice (c) and the center slice (b). (d) and (g) show the 1/g-factor, (e) and (h) show the SNR for full k-space encoded scan, (f) and (i) show the 2D SENSE SNR from 2×2 reduced k-space encoded scan of the center slice and the diagonal slice, respectively. (For interpretation of the references to colour in this figure legend, the reader is referred to the web version of this article.)

After we obtained an optimized design, we simulated a rectangular element coil array for 2D SENSE imaging that was published earlier [4] for comparison. The goal of this simulation was to establish a well-known reference to assess the improvement using the proposed method. The coil geometry of the two designs, the coil sensitivity profile, the 1/g-factor, and the SNR of two selected slices are shown in Figs. 3 and 4. The SENSE imaging performance of the coils are compared and the details are given in Table 1.

With the first optimized design, the mean SENSE SNR improved from 84 to 91. However, most of the improvement was in the periphery of the cylindrical VOI; the uniformity of SENSE SNR did not improve, and the SENSE SNR in the center of the VOI was still low. Therefore, we decided to investigate a different design that would enhance both the SENSE SNR in the center and the SNR uniformity. For this purpose, we assigned greater weight to the SENSE SNR in the center. In the extreme case, we assigned zero weight to the SENSE SNR in the outer 40% of the VOI, and uniform weight 1 to the SENSE SNR in the center 60% of the VOI. In other words, we ignored the outer region of the VOI in the optimization while only optimizing the SENSE SNR in the center 60% of the VOI. With these additional criteria, the optimization algorithm yielded the second optimized design as shown in Fig. 5. The 2D SENSE imaging performance of this coil is also listed in Table 1. This time, the SENSE SNR improved in the center 60% of the VOI (36% of total coil volume) and the variance of SENSE SNR reduced to 0.15, which indicates significant improvement in SNR uniformity was achieved. The noise correlation matrices of the three designs are given in Table 2.

Table 1
2D SENSE Performance of the three RF coil arrays

	The rectangular coil array	The first optimized coil array	The second optimized coil array
Mean SNR_{FULL}	188	203	196
Mean g-factor	1.13	1.11	1.16
Max g-factor	1.30	1.37	1.38
Mean SNR_{SENSE}	84	*91*	85
Variance SNR_{SENSE}	0.27	0.32	*0.15*
Center SNR_{SENSE}	50	40	53

Performance of the three coil arrays in 3D (three dimensional) imaging with 2D SENSE compared by simulation. The first optimized coil array has the highest mean SENSE SNR of 91, and the second optimized coil array has the lowest variance of SENSE SNR of 0.5, which indicates the most uniform SENSE SNR distribution was achieved.

3.2. Coil construction

We built the RF coil array based on the results of the first optimized design (Fig. 4), because the RF coil array was to be used for imaging of the neocortex, and the

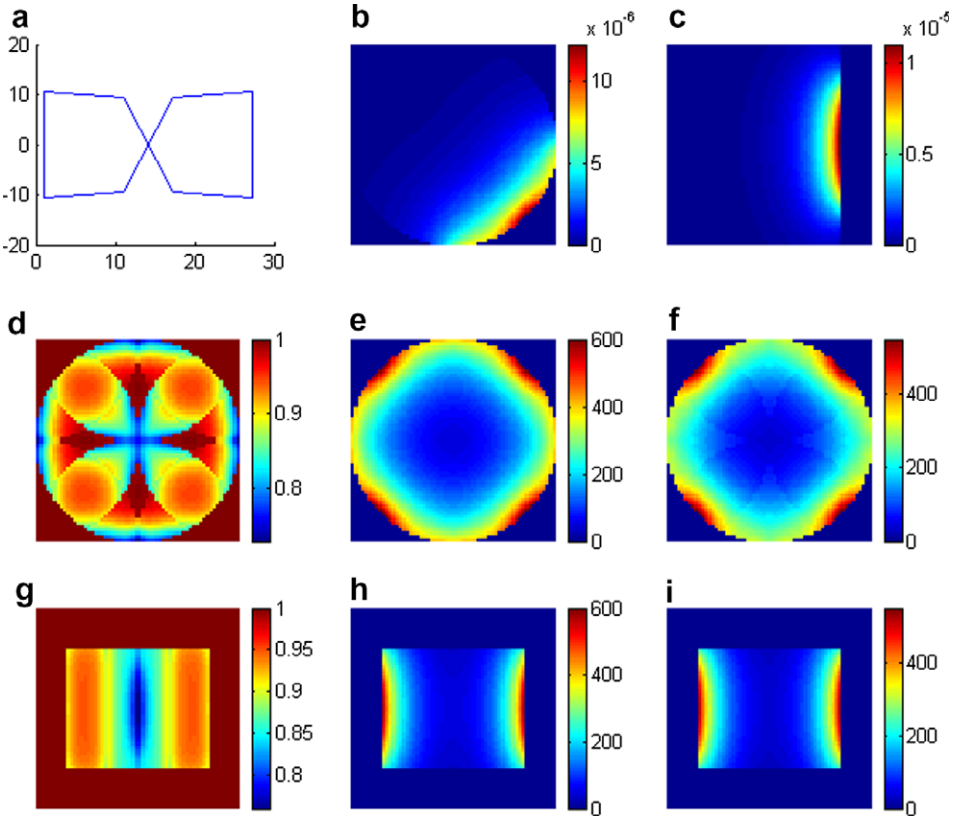

Fig. 4. The first optimized design when $1/SNR_{SENSE}$ was minimized in the full VOI. The geometry of one of the RF coil array elements (a), RF coil sensitivity (b, c), 1/g-factor (d, g), full SNR (e, h) and SENSE SNR (f, i) as explained in Fig. 3.

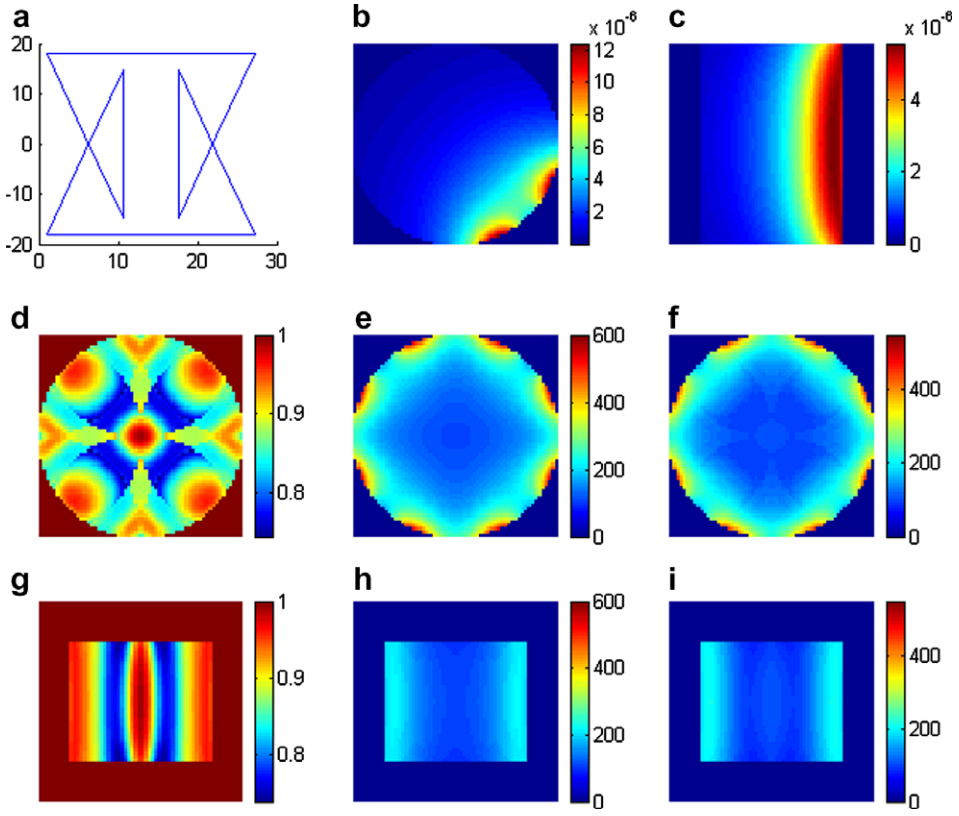

Fig. 5. The second optimized coil design when the center 60% of VOI was given more weighting in the least squares calculations. The geometry of one of the RF coil array elements (a), RF coil sensitivity (b, c), 1/g-factor (d, g), full SNR (e, h) and SENSE SNR (f, i) as explained in Fig. 3.

improved SNR in the outer portion of the VOI is desirable (Fig. 6).

The RF coil array was first etched on a flexible copper clad G10 board and then wrapped around an acrylic tube with a 28 cm diameter. The RF coil array was tuned to 63.73 MHz (the resonance frequency of the 1.5 T Marconi/Philips scanner). The RF coil array was to be used in the receive-only mode, together with a body coil for transmission; so active and passive detuning methods were implemented. To achieve isolation among the 4-channel coils, we first measured the coupling between opposite ele-

Table 2
Noise correlation matrices

$\psi_{\gamma,\gamma'}$		1	2	3	4
The rectangular coil array	1	1.00	0.17	−0.09	0.17
	2	0.17	1.00	0.17	−0.09
	3	−0.09	0.17	1.00	0.17
	4	0.17	−0.09	0.17	1.00
The first optimized coil array	1	1.000	0.002	0.004	0.002
	2	0.002	1.000	0.002	0.004
	3	0.004	0.002	1.000	0.002
	4	0.002	0.004	0.002	1.000
The second optimized coil array	1	1.000	0.25	−0.14	0.25
	2	0.25	1.000	0.25	−0.14
	3	−0.14	0.25	1.000	0.25
	4	0.25	−0.14	0.25	1.000

Comparison of the noise correlation matrices of the rectangular RF coil array and the two optimized RF coil arrays by simulation.

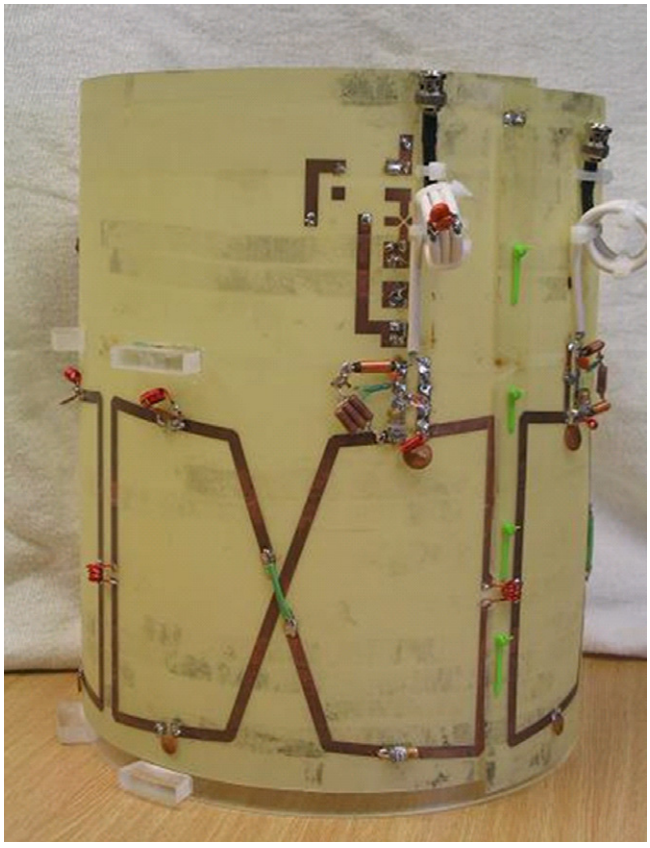

Fig. 6. The home built 4-element RF coil array optimized for 3D imaging with 2D SENSE at 1.5 T.

ment pairs (one pair was detuned while the other pair was measured). We found that the coupling was low for both opposite pairs, with S12 < -20 dB, so there was no need to decouple the opposite channels. However, inductive coupling among adjacent coil elements was strong (S12 > -8 dB), so we used transformer decoupling and achieved S12 better than -16 dB among all the channels. Each channel was then matched to 50 ohm and connected to a preamplifier with 50-ohm input and output impedance. Solenoid baluns were used to isolate the outer shield of the coaxial cable from the coil ground.

3.3. Imaging results

3.3.1. Comparison of RF coil Sensitivity and SENSE SNR

To investigate the optimized coil array for 2D SENSE imaging, we measured the array sensitivity with a uniform phantom. We used the 3D RF-Fast sequence with $20 \times 20 \times 25.6$ cm FOV, $50 \times 64 \times 128$ acquisition matrix, $4 \times 3.125 \times 2$ mm resolution, 30° flip angle, 2.24 ms TE, and 30 ms TR.

The result is shown in Fig. 7. As expected, the measured RF coil sensitivity is in accordance with the simulation results.

We also measured the SNR using the RF coil array for 2D SENSE imaging. We used the 3D RF-Fast sequence with $10 \times 10 \times 25.6$ cm FOV, $50 \times 64 \times 128$ acquisition matrix, $2 \times 1.56 \times 2$ mm resolution, 30° flip angle, 2.24 ms TE, and 30 ms TR for the 2D SENSE imaging with a phase reduction rate of 2×2. To acquire the coil array sensitivity for SENSE reconstruction, two reference data sets were acquired with the same coil array and the body coil using the same sequence with $20 \times 20 \times 25.6$ cm FOV, $50 \times 64 \times 128$ acquisition matrix, $4 \times 3.125 \times 2$ mm resolution, 30° flip angle, 2.24 ms TE, and 30 ms TR.

We followed Bernstein et al. [22] to reconstruct the 2D SENSE images. The body coil sensitivity was used as the target sensitivity function. Therefore, the reconstructed images have the body coil sensitivity weighting, which is relatively uniform.

To measure the noise level we ran the same 2D SENSE sequence consecutively 15 times, which gave us 15 phantom image sets after reconstruction. Then, the standard deviations of every voxel from the 15 image sets were calculated. We used the calculated standard deviation as the noise level as shown in Fig. 8a. Then we divided the signal by the noise level voxel by voxel to get the 2D SENSE SNR (Fig. 8b). Comparison of Fig. 8b with Fig. 4f shows that the simulation sufficiently predicted the 2D SENSE SNR pattern of this RF coil array. The SNR in the outer region is high and uniform, and the SNR in the center region is lower. Since the goal of the design is to improve SNR in the outer portion of the VOI, the average SNR in the outer 60% of the VOI relative to the average SNR in the whole volume is calculated. For the simulation this ratio is 1.31 and for the experiment this ratio is 1.25. Also, average SNRs in 17 small ROIs (marked by the red color in Fig. 9a) relative to the average SNR of the whole VOI are compared between the simulated value and the measured value. Clearly the simulation provided a good prediction of the SNR distribution found in the experiment.

3.3.2. 2D SENSE imaging using a resolution phantom

To further test the RF coil array for 2D SENSE imaging, we acquired 2D SENSE images using a resolution phantom using the same procedure as above. The images are shown in Fig. 10, and it was observed in the reconstructed images that SENSE related artifacts are almost undetectable while the scanning time is reduced by a factor of 4.

4. Discussion

In this paper, we have demonstrated that by using a set of connected metal segments to model a SENSE RF coil array, the performance of this array can be simulated numerically, and computer optimization algorithms can be developed to seek more efficient designs.

When applying the optimization method, our goal was to find the optimum coil given some practical limitations

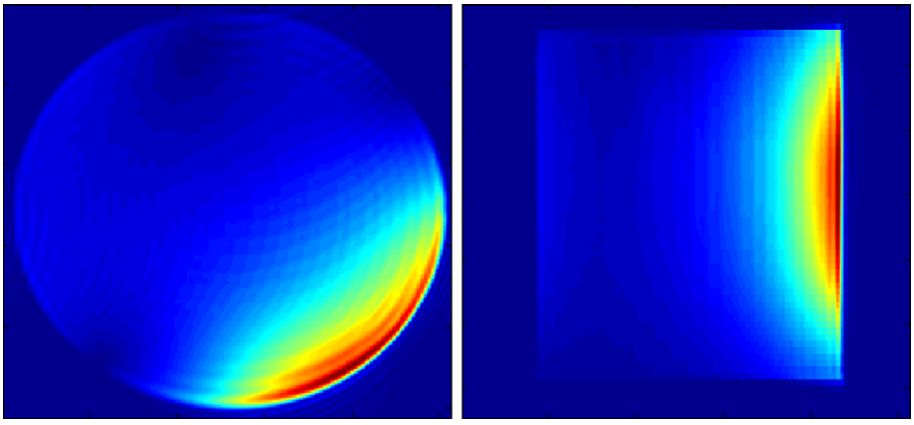

Fig. 7. RF coil sensitivity measured using a uniform phantom. The sensitivity shown here is through the center axial slice (left) and the 45° oblique-sagittal slice (right).

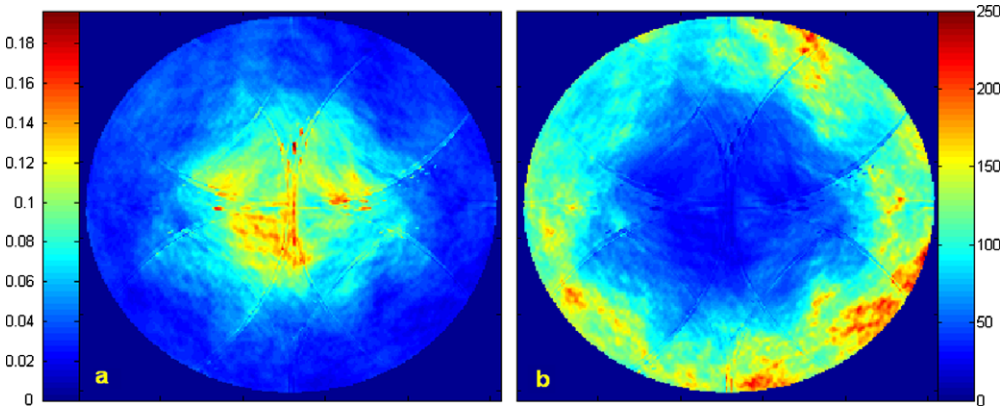

Fig. 8. Noise and SNR measured from a series of 2D SENSE images of a uniform phantom.

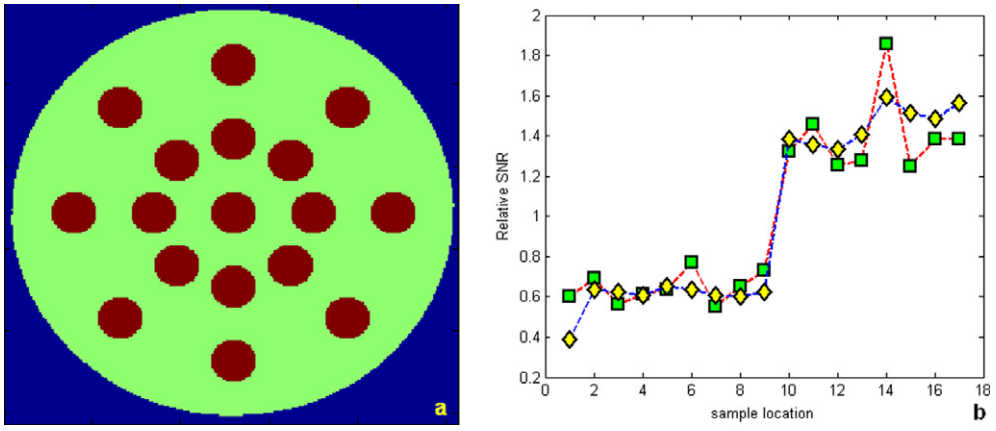

Fig. 9. 17 small ROIs marked by the red color are chosen to compare the simulated and measured SNR (a), the simulated average SNR values of these ROIs are plotted by yellow diamonds and the measured SNR values are plotted by the green square (b). (For interpretation of the references to colour in this figure legend, the reader is referred to the web version of this article.)

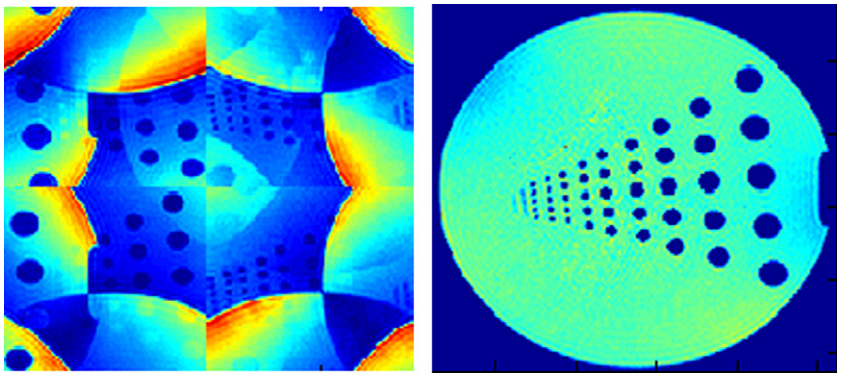

Fig. 10. 2D SENSE images of one selected slice from all four channels before SENSE reconstruction (left), and reconstructed image of the same slice (right).

(number of coils, number of vertices, etc). For this study, the number of coils was fixed. Although the number of coils can be treated as a variable, it is in practice limited by the number of channels provided by the MR console. We chose eight vertices to model each coil because more vertices seemed to be redundant in our previous trial, i.e. when four vertices formed a straight segment in the optimized coil design, the middle two vertices were redundant, but when eight vertices were used there were no redundant vertices found in the optimized coil design. Fewer vertices also reduced the number of unknowns to be solved, resulting in faster optimization.

When the symmetry along the two phase encoding directions was not utilized in our initial trial, the resulting opti-

mized coil designs were still always symmetrical. Therefore this symmetry was enforced to reduce the optimization time in later studies.

The mean SNR_{FULL} and mean SNR_{SENSE} are both improved in our optimized designs compared with the rectangular design. However, the improvements are moderate, except for the uniformity of SNR_{SENSE} with the second optimized coil. The uniformity was greatly improved as seen from the reduced variance of SNR within the defined VOI.

In this study, it was important to assign different weights to different segments of the VOI in the cost function depending on the application. For example, when uniform SENSE SNR distribution is desired throughout the whole volume, one should assign larger weights to the regions in the VOI where the SNR is low with respect to the regions where SENSE SNR is already high.

In the first optimized design, the noise correlation is low among all the channels. Thus this design tends to achieve the best global condition for SENSE imaging, and the average SENSE SNR and g-factor are best. However it does not emphasize the optimization of the SENSE SNR at the worst locations, so the design has the highest variance in SENSE SNR. In the second optimized design, the noise correlation between the channels is high, but the SENSE SNR in the center is the best among all three designs. This design did not try to minimize the noise correlation to achieve the best global SENSE SNR, but instead optimized the SENSE SNR in the worst region and achieved a more uniform SENSE SNR distribution. It should be noted that uniform SENSE SNR may not mean uniform signal intensity or a uniform image. Uniformity of the image intensity in the reconstructed SENSE image can be achieved by using the Target Normalization Method [22] in the SENSE reconstruction.

The RF coil arrays designed in the current work were confined on the surface of a cylindrical former. However, to achieve better performing RF coil arrays, one can use more flexible constraints, such as allowing the coil arrays to grow in a 3D space; e.g. using a helmet shape surface as the inner limit and a cylindrical surface as the outer limit [7]. This might result in a superior design, but also introduce difficulty in constructing the RF coil array.

For magnetic field calculations at relatively low frequencies, we used the Biot–Savart law and ignored loading. This approach is still valid for head coil design at 1.5 T, however at higher frequencies, the electromagnetic field can be calculated by solving the full Maxwell equations using finite-difference time-domain approaches [12,13], finite element approaches [14,15] or integral equation solvers [16], and the same design approach can be adapted accordingly.

References

[1] K.P. Pruessmann, M. Weiger, M.B. Scheidegger, P. Boesiger, SENSE: sensitivity encoding for fast MRI, Magn. Reson. Med. 42 (1999) 952–962.

[2] J.A. de Zwart, P.J. Ledden, P. Kellman, P.V. Gelderen, J.H. Duyn, Design of a SENSE-optimized high-sensitivity MRI receive coil for brain imaging, Magn. Reson. Med. 47 (2002) 1218–1227.

[3] M. Weiger, K.P. Pruessmann, C. Leussler, P. Roschmann, P. Boesiger, Specific coil design for SENSE: a six-element cardiac array, Magn. Reson. Med. 45 (2001) 495–504.

[4] M. Weiger, K.P. Pruessmann, P. Boesiger, 2D SENSE for faster 3D MRI, MAGMA 14 (2002) 10–19.

[5] L.T. Muftuler, G. Chen, O. Nalcioglu, An inverse method to design RF coil arrays optimized for SENSE imaging, Phys. Med. Biol. 51 (2006) 6457–6469.

[6] L.T. Muftuler, G. Chen, O. Nalcioglu, Head RF coil design with surface current density optimization for SENSE imaging, in: Proc. 14th Intl. Soc. Mag. Reson. Med., 2006, p. 2573.

[7] G. Chen, L.T. Muftuler, O. Nalcioglu, 3D RF coil modeling method and its application in optimized SENSE coil design, in: Proc. 14th Intl. Soc. Mag. Reson. Med., 2006, p. 2572.

[8] G. Chen, L.T. Muftuler, O. Nalcioglu, RF coil array optimized for 2D SENSE imaging, in: Proc. 14th Intl. Soc. Mag. Reson. Med., 2006, p. 2574.

[9] S.J. Dodd, H. Merkle, P. van Gelderen, J.H. Duyn, A.P. Koretsky, A 4-channel SENSE optimized array coil for rodent brain imaging at 11.7 T, in: Proc. 13th Intl. Soc. Mag. Reson. Med., 2005, p. 913.

[10] S. Wang, P.J. Ledden, J.H. Duyn, Optimization of 24-channel receive-only coil array for brain imaging at 7.0 tesla by the genetic algorithm, in: Proc. 14th Intl. Soc. Mag. Reson. Med., 2006, p. 2592.

[11] F. Wiesinger, P. Boesiger, K.P. Pruessmann, Electrodynamics and ultimate SNR in parallel MR imaging, Magn. Reson. Med. 52 (2004) 376–390.

[12] J. Jin, Electromagnetic analysis and design in magnetic resonance imaging, CRC Press, Boca Raton, 1998.

[13] A. Taflove, Computational Electrodynamics, the Finite-Difference Time-Domain Method, Artech House, Norwood, 1995.

[14] S. Li, Q.X. Yang, M.B. Smith, RF coil optimization: evaluation of B1 field homogeneity using field histograms and finite element calculations, Magn. Reson. Med. 12 (1994) 1079–1087.

[15] J.M. Jin, The Finite Element Method in Electromagnetics, Wiley, New York, 1993.

[16] R.F. Harrington, Field Computation by Moment Methods, Krieger, Melbourne, FL, 1982.

[17] S.M. Wright, J.R. Porter, An enhanced Biot–Savart law modeling technique for RF coils with unknown current distributions and shields, in: Proc. 2nd Intl. Soc. Mag. Reson. Med., 1994, p. 1131.

[18] T.J. Lawry, M.W. Weiner, G.B. Matson, Computer modeling of surface coil sensitivity, Magn. Reson. Med. 16 (1990) 294–302.

[19] W.R. Smythe, Static and Dynamic Electricity, third ed., McGraw-Hill, New York, 1968.

[20] C. Wang, P. Qu, G.X. Shen, Potential advantage of higher-order modes of birdcage coil for parallel imaging, J. Magn. Reson. 182 (2006) 160–167.

[21] K. Uutela, M. Hamalainen, R. Salmelin, Global optimization in the localization of neuromagnetic sources, IEEE Trans. Biomed. Eng. 45 (1998) 716–723.

[22] M.A. Bernstein, K.F. King, X.J. Zhou, Handbook of MRI Pulse Sequences, Elsevier Academic Press, 2004, p. 536–538.